

Prediction of Postoperative Recurrence-Free Survival in Non-Small Cell Lung Cancer by Using an Internationally Validated Gene Expression Model

Ranjana Mitra¹, Jinseon Lee¹⁰, Jisuk Jo¹⁰, Monica Milani¹, Jeanette N. McClintick³, Howard J. Edenberg³, Kenneth A. Kesler⁴, Karen M. Rieger⁴, Sunil Badve⁵, Oscar W. Cummings⁵, Ahmed Mohiuddin³, Dafydd G. Thomas⁸, Xianghua Luo², Beth E. Juliar⁶, Lang Li⁶, Clementina Mesaros⁹, Ian A. Blair⁹, Anjaiah Srirangam¹, Robert A. Kratzke¹, Clement J. McDonald⁷, Jhingook Kim¹⁰, and David A. Potter¹

Abstract

Purpose: This study was performed to discover prognostic genomic markers associated with postoperative outcome of stage I to III non-small cell lung cancer (NSCLC) that are reproducible between geographically distant and demographically distinct patient populations.

Experimental Design: American patients ($n = 27$) were stratified on the basis of recurrence and microarray profiling of their tumors was performed to derive a training set of 44 genes. A larger Korean patient validation cohort ($n = 138$) was also stratified by recurrence and screened for these genes. Four reproducible genes were identified and used to construct genomic and clinicogenomic Cox models for both cohorts.

Results: Four genomic markers, *DBN1* (drebrin 1), *CACNB3* (calcium channel beta 3), *FLAD1* (*PP591*; flavin adenine dinucleotide synthetase), and *CCND2* (cyclin D2), exhibited highly significant differential expression in recurrent tumors in the training set ($P < 0.001$). In the validation set, *DBN1*, *FLAD1* (*PP591*), and *CACNB3* were significant by Cox univariate analysis ($P \leq 0.035$), whereas only *DBN1* was significant by multivariate analysis. Genomic and clinicogenomic models for recurrence-free survival (RFS) were equally effective for risk stratification of stage I to II or I to III patients (all models $P < 0.0001$). For stage I to II or I to III patients, 5-year RFS of the low- and high-risk patients was approximately 70% versus 30% for both models. The genomic model for overall survival of stage I to III patients was improved by addition of pT and pN stage ($P < 0.0013$ vs. 0.010).

Conclusion: A 4-gene prognostic model incorporating the multivariate marker *DBN1* exhibits potential clinical utility for risk stratification of stage I to III NSCLC patients. *Clin Cancer Res*; 17(9); 2934–46. ©2011 AACR.

Authors' Affiliations: ¹Division of Hematology, Oncology, and Transplantation, Department of Medicine, and Masonic Cancer Center, ²Division of Biostatistics, School of Public Health, University of Minnesota, Minneapolis, Minnesota; ³Department of Biochemistry and Molecular Biology and Center for Medical Genomics, Departments of ⁴Surgery and ⁵Pathology, ⁶Division of Biostatistics, and ⁷Regenstrief Institute for Health Care, Department of Medicine, Indiana University School of Medicine, Indianapolis, Indiana; ⁸Department of Pathology, University of Michigan, Ann Arbor, Michigan; ⁹Center for Cancer Pharmacology, University of Pennsylvania, Philadelphia, Pennsylvania; and ¹⁰Department of Thoracic Surgery, Samsung Medical Center, College of Medicine, Sungkyunkwan University, Samsung Biomedical Research and Samsung Cancer Research Institute, Suwon, Korea

Note: Supplementary data for this article are available at Clinical Cancer Research Online (<http://clincancerres.aacrjournals.org/>).

Corresponding Author: David A. Potter, Division of Hematology, Oncology, and Transplantation, Department of Medicine and University of Minnesota Cancer Center, University of Minnesota, 420 Delaware St. SE, Minneapolis, MN 55455. Phone: 612-625-8933; Fax: 612-625-6919; E-mail: dapotter@umn.edu

doi: 10.1158/1078-0432.CCR-10-1803

©2011 American Association for Cancer Research.

Introduction

The discovery of genomic markers that are prognostic of non-small cell lung cancer (NSCLC) recurrence could change clinical practice by identifying patients who would do well regardless of adjuvant chemotherapy, thus sparing those patients considerable treatment-related toxicities. Recently, patients identified as low-risk for death from lung cancer on the basis of stratification by a 15-gene signature exhibited worse outcomes when treated with adjuvant cisplatin/vinorelbine (1). Many microarray studies of NSCLC gene expression have been performed with the purpose of finding gene markers predictive of overall survival (OS; ref. 2, 3, 4, 5, 6), but few individual genes are reproducible.

Although earlier microarray studies successfully identified gene markers associated with OS, in some cases independent of stage, some studies did not distinguish between

Translational Relevance

Lung cancer is a global problem, but the validation of prognostic genomic markers for recurrence-free survival (RFS) of lung cancer patients may be influenced by local differences in population genetics and environmental factors, including tobacco exposure, diet, and exercise. We hypothesized that comparison of 2 geographically distant and demographically distinct patient cohorts could facilitate the identification and validation of reproducible genomic markers associated with RFS, by eliminating genomic markers that vary between populations. Four genes associated with recurrence in an American training cohort were also identified in a larger Korean validation cohort. One gene, *DBN1*, was multivariate. Genomic and clinico-genomic modeling using these genes risk-stratified both cohorts and stage I to II patients of the validation cohort ($P < 0.0001$). These 4 internationally validated recurrence-associated genes are strong candidates for broader analysis in larger patient cohorts, and likely will contribute to personalized lung cancer management strategies in the multi-disciplinary lung cancer clinic.

death from NSCLC and other causes. Lung cancer markers linked to survival alone exhibit limited clinical utility, because there are significant competing causes of mortality including postoperative mortality (7, 8), the occurrence of second primary cancers including second primary lung cancer, cardiovascular disease, and chronic obstructive pulmonary disease (COPD). Among stage I NSCLC patients, 5-year disease-specific survival is 77% for pT1N0M0 patients and 62% for pT2N0M0 patients (9), while 5-year OS is 67% and 57% for these groups (10). This comparison indicates that even for stage I patients there is a significant death rate from competing causes of death. Recently, there has been an emphasis on disease-specific survival, which has been more helpful (1). Another approach is to study recurrence-free survival (RFS), which has led to significant progress in identification of genomic markers that are associated with lung cancer-specific outcomes (11, 12). Although these studies have led to identification of multivariate gene groups, to the best of our knowledge, they have not led to the discovery of single gene multivariate markers for RFS, whereas pT (9) and pN1 stage (13) are multivariate.

An as yet unrealized goal is to develop stage-independent genomic models for NSCLC that are prognostic for RFS and reproducible between differing patient populations. This goal, if accomplished, would make it possible to predict the likelihood of recurrence within 5-year of surgery based solely on genomic markers, thus giving the patient and oncologist information to make adjuvant therapy decisions that are related to patient's individual tumor biology rather than stage (I–III). This type of model would be very useful

clinically, because patients seen in the NSCLC clinic exhibit a wide range of stages, but may exhibit personalized risk that may differ from that predicted by stage alone. To achieve this goal, reproducible multivariate genomic markers for RFS are needed. Most studies are internally validated by dividing a relatively homogeneous patient cohort, such as one consisting of North American patients, the majority of whom are current or former smokers, into smaller test and larger validation sets. These studies suffer from demographic and geographic similarity of the two populations. Recent studies have successfully identified genomic markers associated with RFS; nonetheless, the lead genomic markers derived within an exclusively North American or Asian patient cohorts are not generally reproducible between demographically distinct and geographically distant populations (11, 12). Differences between genomic markers for RFS may be related to chance or reflect differing mechanisms of cancer recurrence. Differences in recurrence patterns between distinct populations could relate to genetics or interaction of genetics with diet, exercise, and second hand smoke exposure. Although much can be learned about cancer outcome disparities by studying genomic markers within specific racial or ethnic groups, much can also be learned about what is similar between differing groups. Genomic markers that remain the same between differing patient groups are therefore more likely to be broadly useful and independent of confounding factors. Our hypothesis is that improved reproducibility of genomic markers can be achieved by identifying markers that are reproducible between demographically distinct and geographically distant populations.

A novel approach is to identify genomic markers that are of univariate significance in a small training set and then retest them for univariate or multivariate significance in a larger validation group that is demographically distinct. We therefore took a group of 44 lead genomic markers for RFS from a small American training group (stages I–III) and found 4 genes that also exhibited either univariate or multivariate significance in a larger Korean validation group (11). These 4 genomic markers were strongly associated with recurrence in both groups and resulted in a genomic model that was prognostic for recurrence independent of clinical variables, including stage and histology.

Materials and Methods

Training set patients

This study was approved by the Indiana University Purdue University at Indianapolis (IUPUI)/Clarian Institutional Review Board (IRB; no. 0201-58), and the banking of tissue was performed under a separate protocol approved by the same IRB (no. 9401-17; IU-Lilly Tissue Bank). A longitudinal database of consented patients undergoing NSCLC resection with curative intent from July 12, 1999, to January 2, 2002, was searched for banked NSCLC tumor tissue with sufficient tumor content. The tumor resections in the single institution training set were

performed at Indiana University by 2 thoracic surgeons who used consistent procedures for lobectomy or pneumonectomy during the period of the study (8, 14). The lobectomy/pneumonectomy procedure involved ligation of the vein leading to the tumor-containing lobe or lung before arterial ligation. All patients had complete peribronchial and mediastinal lymph node dissections. Patients treated on this study were subsequently followed by the multidisciplinary Thoracic Oncology Program at Indiana University.

All patients ($n = 27$) with stage Ia to IIIB NSCLC, who were evaluable for recurrence at 2 years of follow-up after surgery were included in the study. The median follow-up time for the recurrence-free patients was 57 months. NSCLC recurrence, if suspected, was histologically confirmed. All patient-related data were deidentified by the tissue bank staff so that the investigators could access only coded frozen tissue specimens, coded paraffin slides, and relevant variables for multivariate analysis that were associated with the code number for the patient.

While none of the patients in the training set received adjuvant chemotherapy, one recurrent patient and 2 non-recurrent patients received carboplatin-based chemotherapy as neoadjuvant treatment. One recurrent patient (no. 11) received chemotherapy 8 months before resection, having participated in a phase II study of paclitaxel/carboplatin and cetuximab. The same patient was continued on cetuximab at the time of recurrence, which was 8 months following resection. One nonrecurrent patient (no. 13) received paclitaxel/carboplatin 2 months before resection. Another nonrecurrent patient (no. 21) received paclitaxel/carboplatin for 2 cycles before resection, which was performed 7 weeks after initiation of chemotherapy.

Pathology

NSCLC tumor histology was confirmed by hematoxylin/eosin (H&E) staining of associated tissue blocks. The frozen samples included in the study ranged from 90% to 40% tumor tissue with a mean of $59\% \pm 11\%$ SD. Of the 30 specimens that were available for study, 3 were rejected because they either contained mainly stroma or necrosis, or exhibited less than 40% tumor epithelium. The percentage of malignant cells in the frozen tumor specimen could not be determined definitively from the single 5 micron frozen section, in part, because of the difficulty of completely counting the admixture of interspersed normal stromal, endothelial cells, and immunocytes, which were much smaller than the tumor cells.

RNA isolation and purification

Tumors were collected by a tissue procurement service in the operating room and stored in liquid nitrogen immediately following resection and remained frozen until RNA isolation was performed. Specimens were removed from liquid nitrogen, transported on dry ice to the laboratory and homogenized using a Polytron homogenizer (Brinkmann Instruments) in ice-cold Trizol reagent (Gibco BRL). RNA was extracted with chloroform and precipitated using

isopropanol with glycogen as carrier. The RNA pellet was washed in 75% ethanol and resuspended in DEPC-treated MilliQ water. The RNA was diluted in a guanidinium thiocyanate-containing RLT buffer (Qiagen Sciences, Inc.) and further purified using a silica-gel-based membrane in RNeasy MinElute spin columns. The RNA quality was confirmed by electrophoresis on a 1% nondenaturing agarose gel or by Agilent Bioanalyser, which revealed intact 18 and 28S rRNA in all samples. UV spectroscopy ($A_{210}-A_{350}$) was performed to confirm RNA purity; the A_{260}/A_{280} ratio was 1.99 to 2.00 for all samples.

RNA hybridization

cDNA was prepared from total RNA (10 μ g) using the Superscript Choice system (Gibco-BRL). A T7-(dT) oligonucleotide primer was used for first strand synthesis. Double-stranded cDNA was purified by phenol/chloroform extraction and the Phase Lock Gel method (Eppendorf-5 Prime). Biotin-labeled cRNA was synthesized using a BioArray RNA Amplification and Labeling kit (ENZO), cleaned and fragmented (15). The cRNA was biotin labeled and hybridized on U133A GeneChip arrays for 17 hours (45°C) in an Affymetrix GeneChip 640 Hybridization Oven (Affymetrix). Washing and staining of the chips were performed using the Affymetrix GeneChip Fluidics Station 400. Arrays were scanned in an HP GeneArray Scanner (Hewlett Packard), and data were analyzed with Affymetrix Microarray Suite v5.0 software (MAS5).

Microarray analysis of discriminatory genes

Probes that were not detected as "present" in at least half of the samples using the standard MAS5 parameters were removed from analysis (16, 17). The remaining probes were analyzed using Welch's *t*-test, assuming unequal variance, on the \log_2 transformed MAS5 signals. The Affymetrix chip for one patient, sample no. 26, was damaged; consequently, this patient was deleted from the gene analyses.

Quantitative reverse transcriptase PCR

First strand cDNA synthesis was performed using SuperScript III reverse transcriptase (RT; Invitrogen Corp.) with total RNA (5 μ g) and oligodT₁₂₋₁₈ primer. The reaction mix was diluted (1:12.5) and used for quantitative PCR (qPCR) analysis. The primers and probes used for the PCR were purchased from Applied Biosystems (Foster city). The probes used for *DBN1* (Hs00365623_m1, exon boundary 9-10), *PP591* (Hs00611011_m1, exon boundary 5-6), *CCND2* (Hs00277041_m1, exon boundary 1-2), and *CACNB3* (Hs00167873_m1, exon boundary 9-10) were all Fluorescein Amidite (FAM) labeled. FAM labeled glyceraldehyde-3-phosphate dehydrogenase (GAPDH) probes (433376F) was used in separate experiments to normalize the C_t value between the samples. The Applied Biosystems master mix was used for the qPCR reaction and the manufacturer's instructions were followed. The qPCR reactions were performed in a I-Cycler (BioRad laboratories) at 50°C (2 minutes), 95°C (10 minutes) followed by 40 cycles of

consisting of 95°C (15 seconds) and 60°C (1 minute) steps. The reactions were performed in triplicate and the GAPDH C_t values were subtracted from the raw sample C_t values to get the corrected C_t , which was converted into the relative RNA amount using the formula ($2^{-(\text{corrected } C_t)}$). All the 27 patient samples were used for qPCR analysis.

Hierarchical clustering analysis of genes associated with recurrence

For hierarchical clustering, 51 probe sets that differed between the groups ($P < 0.001$) were selected. The \log_2 transformed MAS5 signals were normalized [(signal-mean)/SD] and then arrays were clustered using the hierarchical clustering function of Partek Genomics Suite, version 6.3 2007 (Partek, Inc.), with Euclidean distance and average linkage. Pearson's dissimilarity and average linkage were used to cluster the probe sets. Normalization was performed on each probe set to ensure that no individual probe set would have undue influence on the clustering.

Validation set patients

The validation set consisted of 138 patients ($n = 138$) from Samsung Medical Center. Of 138 patients, 69 exhibited no recurrence following surgery (group NR) and 69 patients exhibited recurrence after surgery (group R). The details of the patients of this validation set are described in Lee and colleagues, 2008 (11). The patients were a mix of different NSCLC stages, established by pathologic staging after surgery: 64%, 17%, and 19% were stages I, II, and III, respectively. The tumor node metastasis (TNM) staging of the patients was widely distributed: 17% patients were pT1 stage, 68% pT2, 7% pT3, and 7% pT4. Most of the patients had no nodal involvement (pN0, 71%), while 20% were pN1 and 9% were pN2. Of the total, 63 patients had adenocarcinoma and 75 patients had squamous cell carcinoma. The microarray data obtained was processed using gene chip robust multiarray average (GCRMA) normalization (18) with perfect match (PM) and perfect match/mismatch (PM/MM) modeling.

Among the 69 nonrecurrent patients, 3 received adjuvant combination chemotherapy. Specifically, 1 patient received a combination of fluorouracil, leucovorin, ifosfamide, and dexamethasone, another patient received combination of etoposide and dexamethasone, and a third patient received a combination of cisplatin and paclitaxel. Nine of the recurrent patients received different adjuvant chemotherapy or biologically targeted regimens including: gefitinib, etoposide/dexamethasone, cisplatin/paclitaxel, cisplatin/etoposide/dexamethasone, and docetaxel/cisplatin/dexamethasone/gemcitabine.

Clinical, genomic, and clinicogenomic models of RFS in the training set

The objective was to derive 3 models for RFS: models based solely on patient characteristics (i.e., clinical model), solely on gene expression levels (i.e., genomic model), and on both (i.e., clinicogenomic model). To

model RFS outcomes in the training set, multivariate analyses were performed using a stepwise Cox proportional hazards model on the 27 patients (stage I–III). For the clinical model, patient characteristics including age, sex, race, and smoking history were considered. Smoking history was categorized as: current smoker (C, defined as smoking <1 year before surgery), former smoker (F, defined as quit >1 year before surgery), and never smoker (N). For each of the models, a subsequent Cox score was calculated and dichotomized at its median value into low- and high-risk groups. The RFS curves were estimated using the Kaplan–Meier method and compared by log-rank test. The variables used for the clinical model of the training set were: histology, pathologic stage (pStage), sex, race, and smoking. For the genomic and clinicogenomic models the natural logarithm of gene expression levels determined by qPCR was included, using the genes *DBN1*, *FLAD1* (*PP591*; flavin adenine dinucleotide synthetase), *CACNB3*, and *CCND2*, which were identified as being differentially expressed in both the training and validation sets. Median value of the Cox score was determined as previously described (11) and was used to dichotomize the patients into low- and high-risk groups for Kaplan–Meier plots. The equations used for the modeling are given in the Figure 2 legend. The SAS program codes used to derive the models are provided in the Supplementary Material (SAS codes).

Genomic and clinicogenomic RFS models of the validation set

Genomic and clinicogenomic models for the stage I to III patients of the validation set were developed similar to a prior study of the same cohort, for which the clinical model has already been published (11). The genomic markers used for the validation set model were: *DBN1*, *FLAD1* (*PP591*; flavin adenine dinucleotide synthetase), *CACNB3*, and *CCND2*. For the validation set, there were several Affymetrix probes for each gene: 2 for *DBN1*, 2 for *CACNB3*, 5 for *CCND2*, and 2 for *FLAD1* (Supplementary Table S2). To optimize the model, all the probe combinations were considered ($2 \times 2 \times 5 \times 2 = 40$). Single Affymetrix probes were selected for each gene using a stepwise parameter method (11) that allowed selection of an optimized model of 4 unique probes (Supplementary Table S2). To develop the clinicogenomic model for the validation set, the same stepwise parameter selection was also used for filtering of clinical variables. Pathologic T stage ($P = 0.0003$) and pathologic N stage ($P = 0.0038$) were identified as being of utility among the considered variables, whereas age, gender, cell type, tumor size, smoking status, and tumor differentiation were not.

Median value of the Cox score was determined as previously described (11) and was used to dichotomize the patients into low- and high-risk groups for Kaplan–Meier plots. The equations used for the modeling are given in the Figure 2 legend. The SAS program codes used to derive the models are provided in the Supplementary Material (SAS codes).

Genomic and clinicogenomic RFS modeling of stage I and II patients in the validation set

Stage I to II patients of the validation set were selected for Cox analysis. The genomic markers used for the genomic modeling were those described above (*DBN1*, *FLAD1*, *CACNB3*, and *CCND2*). The clinicogenomic model incorporated the genomic information with additional pT and pN stage data. The Cox equations used for the modeling are given in Figure 2 legend. The SAS program codes used to derive the models are provided in the Supplementary Material (SAS codes). Due to the relatively small number of patients, this type of analysis was not performed on the training set.

Genomic and clinicogenomic OS modeling of validation set

Stage I to III patients of the validation set were included in this Cox analysis. All the deaths included in this analysis are death due to lung cancer, including complications associated with lung cancer (disease-specific OS). To optimize the OS model, a Cox proportional hazards regression model with stepwise parameter selection method was developed. The Cox equations used for the modeling are given in Figure 3 legend. The SAS program codes used to derive the models are provided in the Supplementary Material (SAS codes). Due to the relatively small number of patients, this analysis was not performed on the training set.

Results

American patient training set

The training set of patients accrued at the Indiana University Thoracic Oncology Program consisted of 27 patients with stage Ia to IIIB NSCLC who were evaluable for recurrence at 2 years of follow-up. All histologies of NSCLC were included. This patient cohort was reflective of a broad patient population seen in an American academic medical center without selection for histology or stage. This approach could be useful because genomic markers derived from this type of study could potentially be applied to clinical decision-making in a general thoracic oncology practice. There were 11 patients who experienced recurrence within 2 years of resection (group R) and 16 patients who did not (group NR). Patient characteristics, including stage of disease, recurrence status, histology, age at surgery, smoking history, survival after surgery, time to recurrence (TTR), gender, and adjuvant therapy are described in Table 1. The majority of the NSCLC patients exhibited adenocarcinoma histology ($n = 19$). Mean age of the patients at operation was 61.8 (SD = 12.8) years (range 34–81 years).

The median TTR of group R was 12 months and the median OS was 20 months. This study had a 57-month median follow-up and the 2-year cut-off captured 81% of the recurring patients. Among the NR group, 19% of the patients recurred after 2 years, the recurrences being at 32, 50, and 53 months and these patients were still alive at the

time of data collection closure. Age at operation, race, gender, and smoking status were analyzed in conjunction with gene expression data in subsequent Cox multivariate analysis (see below).

Genomic markers associated with NSCLC recurrence in the training set

To identify genes that were differentially expressed in recurring patients, genomic microarray analysis of tumor gene expression was performed by Affymetrix U133A chip hybridization. Candidate genomic recurrence markers (Table 2) were identified from 12,956 evaluable probes in the microarray by statistical analysis of \log_2 -transformed signals (Welch's t -test; $P \leq 0.001$). This analysis resulted in 51 probes corresponding to 44 genes that were differentially expressed between the R and NR groups (Table 2; raw data available at Geo database; GSE9971; Supplementary Table S1).

Hierarchical clustering analysis of training set genes associated with NSCLC recurrence

Hierarchical clustering using the 51 probes associated with recurrence separated the training set patients exhibiting recurrence. Based on recurrence or not at 2 years of follow-up, this clustering identified 3 subgroups of genes exhibiting upregulation and one exhibiting downregulation in recurrence (Fig. 1). The most statistically significant markers upregulated in recurrence were, in order of significance by Welch's t -test, *FLJ20343*, *DKFZp566O084*, *CACNB3*, *CYP3A5*, and *DBN1* (Table 2). The first 3 markers were associated with 1 cluster of genes upregulated in patients exhibiting recurrence (group 1), while *CYP3A5* was associated with a second cluster (group 2), and *DBN1* with a third (group 3). Genes in groups 1 to 3 were associated with a broad range of t -test values (ranging from 0.001 to 0.00001). The most statistically significant markers that were downregulated in recurring patients were, in order of significance, *C14orf118*, *STAT2*, *ATF7IP*, *HIPK3*, and *HLA-DOA* (Table 2) and this group clustered together (group 4). Group 4 exhibited a smaller distribution of t -test values (ranging from 0.0009 to 0.00008), consistent with the larger size of this group.

Screening of a Korean patient validation set for concordance of candidate genomic markers

We hypothesized that screening of a geographically distant and demographically distinct patient population for recurrence-associated genomic markers would lead to the identification of more reproducible genes for the study of NSCLC prognosis. To find a distinct and larger validation set, the GEO database was screened for NSCLC studies with similar stage grouping and no selection based on histology, performed on a similar genomics platform. A Korean study of NSCLC recurrence-associated genomic markers, GSE8894, met the criteria for comparison with the American training set and was probed for genomic markers associated with recurrence common to both sets (11). The Kaplan–Meier curve for the Korean patients exhibited

Table 1. Description of training set patients

		Training set (n = 27)	
Age at operation, y	Mean	61.8 (SD = 12.8)	
	Range	34–81	
Gender	Male	15	55.5%
	Female	12	44.5%
Smoking history	Never smoker	5	18.5%
	Former smoker	14	51.9%
	Current Smoker	8	29.6%
Histology	Adenocarcinoma (ADC)	18	66.7%
	Squamous carcinoma (SQC)	3	11.1%
	Other	6	22.2%
Histologic differentiation	Well differentiated	25	92.6%
	Poorly differentiated	2	7.4%
Stage	IA	5	18.5%
	IB	10	37.0%
	IIA	1	3.7%
	IIB	3	11.1%
	IIIA	5	18.5%
	IIIB	2	7.4%
	Not known	1	3.7%
	T	1	7
N	2	15	55.6%
	3	1	3.7%
	4	1	3.7%
	Not known	3	11.1%
	0	16	59.3%
M	1	3	11.1%
	2	4	14.8%
	3	1	3.7%
	Not known	3	11.1%
	0	9	33.3%
TTR (number of patients)	X	13	48.1%
	Not known	5	18.5%
	0–12 months	6	22.2%
	13–24 months	5	18.5%
	25–36 months	1	3.7%
	37–48 months	0	0%
Not recurred (up to max follow-up of 67 months)	49–60 months	2	7.4%
	13	48.1%	
Overall survival, months	0–12	2	7.4%
	13–24	4	14.8%
	25–36	2	7.4%
	37–67 (max follow-up)	19	70.4%
	Adjuvant therapy	Neoadjuvant	3
	Adjuvant	0	0%

a median disease-specific survival time of 69.4 months and a 5-year survival percentage of 56.2%, comparable to but perhaps slightly shorter than North American patients with resected NSCLC (ref. 9; Supplementary Fig. S1).

Each of the 44 genes identified in the American training set was tested in the Korean data set for significance by univariate and multivariate Cox analysis. The 4 genes that were most significant by univariate Cox analysis were, in

order of significance, *DBN1*, *FLAD1* (*PP591*), *CACNB3*, and *CCND2* (Table 3). The first 3 genes exhibited *P* values less than 0.05 and the fourth, exhibiting a *P* value of 0.08, was retained for model building. By multivariate analysis, only *DBN1* exhibited significance (*P* = 0.0095; Table 3). Nonetheless, 2 of the genes approached multivariate significance, *FLAD1* (*P* = 0.0720) and *CCND2* (*P* = 0.0713), while *CACNB3* did not (*P* = 0.1813; Table 3).

Table 2. Differentially expressed genes in recurrent NSCLC (group R) compared to nonrecurrent NSCLC (group NR)—differential analysis based on *P* values less than 0.001

Gene symbol	Source id	Fold change	Welch's <i>t</i> -test log (signal)	Description
<i>CYP3A5</i>	205765_at	18.66	1.30E-04	Cytochrome P450, family 3, subfamily A, polypeptide 5
<i>DPM3</i>	219373_at	1.87	4.60E-04	Dolichyl-phosphate mannosyltransferase polypeptide 3
<i>NES</i>	218678_at	1.85	2.20E-04	Nestin
<i>TACSTD1</i>	201839_s_at	1.84	5.80E-04	Tumor-associated calcium signal transducer 1
<i>DECR1</i>	202447_at	1.74	1.50E-04	2,4-dienoyl CoA reductase 1, mitochondrial
<i>DBN1</i>	202806_at	1.71	6.40E-04	Drebrin 1
<i>KIAA1598</i>	221802_s_at	1.62	5.30E-04	KIAA1598
<i>CACNB3</i>	34726_at	1.58	1.10E-04	Calcium channel, voltage-dependent, beta 3 subunit
<i>PP591</i>	212541_at	1.56	8.40E-04	FAD-synthetase
<i>PSMD4</i>	200882_s_at	1.56	6.20E-04	Proteasome 26S subunit, non-ATPase, 4
<i>DNAJB12</i>	202866_at	1.52	3.50E-04	DnaJ (Hsp40) homolog, subfamily B, member 12
<i>MAN2A2</i>	202032_s_at	1.52	2.60E-04	Mannosidase, alpha, class 2A, member 2
<i>D2LIC</i>	203763_at	1.51	0.001	Dynein 2 light intermediate chain
<i>DKFZp566O084</i>	220690_s_at	1.51	7.00E-05	DKFZP566O084 protein
<i>FLJ20343</i>	217964_at	1.46	1.00E-05	Hypothetical protein FLJ20343
<i>BCAP31</i>	200837_at	1.45	3.00E-04	B-cell receptor-associated protein 31
<i>SMBP</i>	217758_s_at	1.42	8.10E-04	SM-11044 binding protein
<i>ECHS1</i>	201135_at	1.39	8.80E-04	Enoyl Coenzyme A hydratase, short chain, 1
<i>SCRIB</i>	212556_at	1.38	5.00E-04	Scribbled homolog
<i>SUPV3L1</i>	212894_at	1.35	8.40E-04	Suppressor of var1, 3-like 1
<i>XPNPEP1</i>	209045_at	1.35	9.90E-04	X-prolyl aminopeptidase 1
<i>C10orf119</i>	217905_at	1.33	4.00E-04	Chromosome 10 open reading frame 119
<i>ACTR1A</i>	200721_s_at	1.32	3.30E-04	ARP1 actin-related protein 1 homolog A
<i>PSMB4</i>	202244_at	1.23	9.80E-04	Proteasome subunit, beta type, 4
<i>TEX27</i>	218020_s_at	-1.19	5.90E-04	Testis expressed sequence 27
<i>MLL</i>	212076_at	-1.24	6.50E-04	Myeloid/lymphoid or mixed-lineage leukemia
<i>ENO1</i>	216554_s_at	-1.28	4.50E-04	Enolase 1
<i>C6orf69</i>	214849_at	-1.35	8.30E-04	Chromosome 6 open reading frame 69
<i>SPAG9</i>	212470_at	-1.37	2.40E-04	Sperm-associated antigen 9
<i>STK17B</i>	217503_at	-1.37	6.50E-04	Serine/threonine kinase 17b
<i>FLJ10996</i>	219774_at	-1.38	9.20E-04	Hypothetical protein FLJ10996
<i>C14orf118</i>	219720_s_at	-1.41	8.00E-05	Chromosome 14 open reading frame 118
<i>TBC1D5</i>	201815_s_at	-1.41	2.20E-04	TBC1 domain family, member 5
<i>CLN5</i>	204085_s_at	-1.43	9.10E-04	Ceroid-lipofuscinosis, neuronal 5
<i>AHCYL1</i>	207464_at	-1.45	4.10E-04	S-adenosylhomocysteine hydrolase-like 1
<i>STAT2</i>	205170_at	-1.48	1.10E-04	Signal transducer and activator of transcription 2
<i>ATF7IP</i>	218987_at	-1.52	1.30E-04	Activating transcription factor 7 interacting protein
<i>CD44</i>	210916_s_at	-1.62	4.20E-04	CD44 antigen
<i>HIPK3</i>	210148_at	-1.72	1.80E-04	Homeodomain interacting protein kinase 3
<i>HIPK3</i>	207764_s_at	-1.85	1.40E-04	Homeodomain interacting protein kinase 3
<i>CD44</i>	204490_s_at	-1.88	2.50E-04	CD44 antigen
<i>CCND2</i>	200952_s_at	-1.89	1.90E-04	Cyclin D2
<i>CD44</i>	209835_x_at	-1.99	5.40E-04	CD44 antigen
<i>TRA@</i>	209671_x_at	-2.1	3.10E-04	T cell receptor alpha locus
<i>CD44</i>	212014_x_at	-2.12	8.80E-04	CD44 antigen
<i>HLA-DOA</i>	206313_at	-2.2	1.60E-04	Major histocompatibility complex, class II, DO alpha
<i>SOD2</i>	221477_s_at	-2.25	6.60E-04	HepG2 3' region Mbol cDNA, clone hmd2a08m3
<i>SOD2</i>	216841_s_at	-2.52	7.40E-04	Superoxide dismutase 2, mitochondrial
<i>SOD2</i>	215223_s_at	-2.77	8.80E-04	Superoxide dismutase 2, mitochondrial
<i>CCND2</i>	200951_s_at	-3.49	4.50E-04	Cyclin D2
<i>CXCL13</i>	205242_at	-5.31	4.00E-04	Chemokine (C-X-C motif) ligand 13

NOTE: Affymetrix source id is indicated because of the identification of multiple Affymetrix probes for several genes, including *CD44*, *SOD2*, *HIPK3*, and *CCND2*.

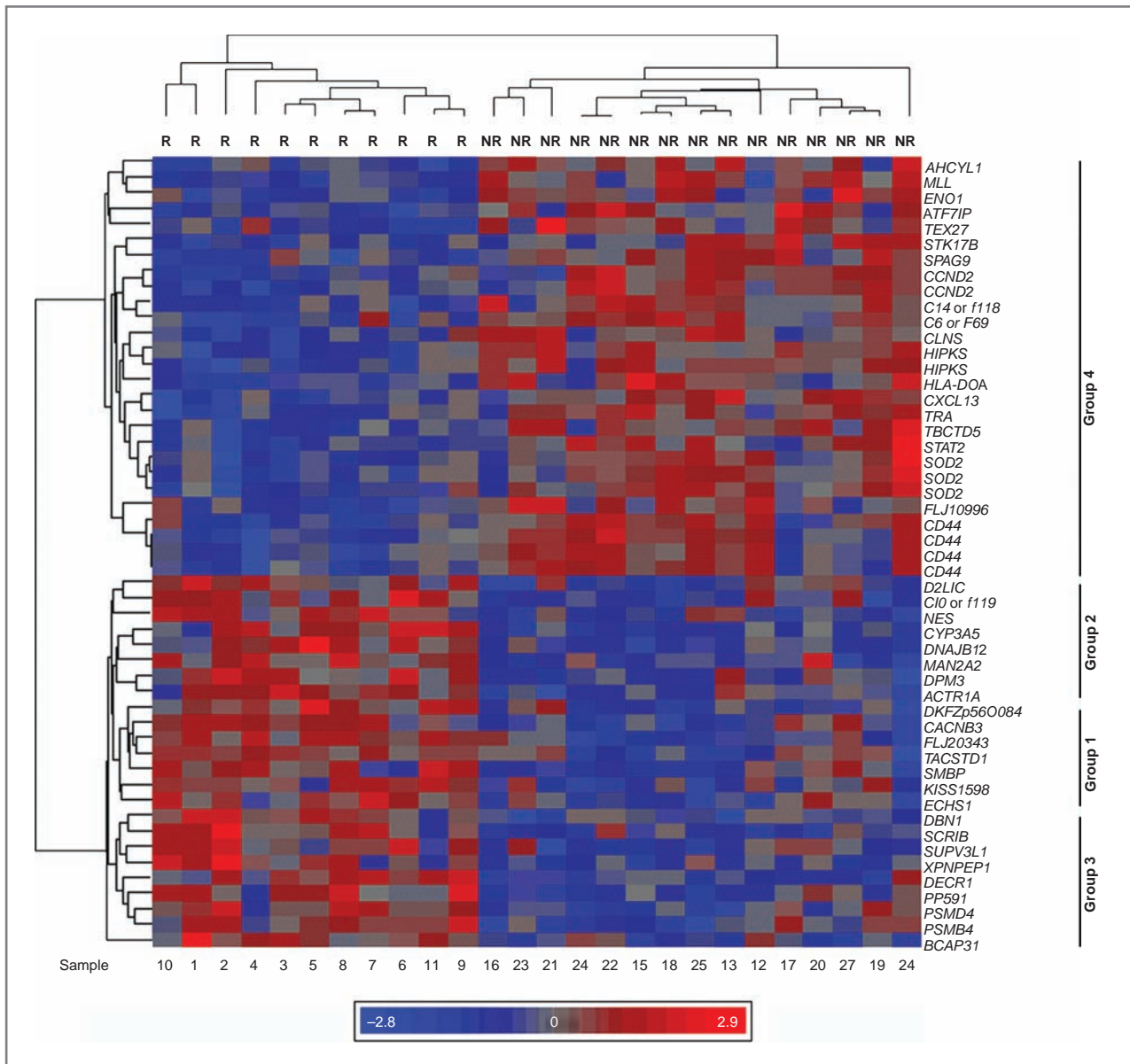


Figure 1. Gene expression profile and hierarchical clustering separating the recurrent and nonrecurrent groups on the basis of discriminatory genes. Twenty six evaluable tumors were clustered hierarchically on the basis of 51 probes corresponding to 44 genes, using Partek Genomics Suite v6.3. The dendrograms of individual patient samples and overall patterns of gene expression data are exhibited. The recurrent group is labeled R and nonrecurrent NR. Individual tumor specimen numbers are indicated at the bottom of the figure and the tumor specimen dendrogram is given along the top. Gene symbols are indicated on the right side of the figure and relatedness of gene expression is indicated by the dendrogram on the left side of the figure. The clustering is of \log_2 transformed Affymetrix MAS5 signals. Red color indicates increased expression and blue color lower, relative to the mean level of gene expression, indicated in gray. The color scale indicates the mean \log_2 expression level above (red) and below (blue) the mean of all genes (gray), over a range of 2.9 \log_2 units above and below the mean.

These results indicate that *DBN1* is potentially of value as a multivariate marker and the combination of the 4 genes was effective in model building (see below).

Confirmation of *DBN1*, *CACNB3*, *FLAD1* (*PP591*), and *CCND2* expression in the training set by qPCR

The utility of prognosis-associated genes identified by microarray analysis is increased if they are also assayable by

qPCR (11). Increased expression of the *DBN1*, *CACNB3*, and *FLAD1* (*PP591*) genes in the recurrent NSCLC tumors was confirmed in the training set by qPCR (Table 4). Decreased expression of *CCND2* in the recurring patients of the training set approached, but did not reach, statistical significance (Table 4). These expression values were used to perform subsequent Cox regression analysis of the training set.

Table 3. Validation of genes using Cox analysis

Gene symbol	Probe	HR	95% CI for HR	Cox analysis <i>P</i>
A-Univariate Cox analysis				
<i>DBN1</i>	202806_at	1.743	1.238, 2.453	0.0014
<i>FLAD1 (PP591)</i>	212541_at	1.567	1.064, 2.307	0.0229
<i>CACNB3</i>	34726_at	1.421	1.025, 1.968	0.0347
<i>CCND2</i>	200952_at, 200951_s_at	0.296	0.075, 1.163	0.0813
B-Multivariate Cox analysis				
<i>DBN1</i>	202806_at	1.565	1.116, 2.195	0.0095
<i>FLAD1 (PP591)</i>	212541_at	1.422	0.969, 2.088	0.072
<i>CACNB3</i>	34726_at	1.267	0.896, 1.792	0.1813
<i>CCND2</i>	200952_at, 200951_s_at	0.303	0.083, 1.109	0.0713

Clinical, genomic, and clinicogenomic modeling of the training and validation sets

A clinical model of the training set was performed, based on histology, pStage, sex, race, and smoking history (Fig. 2A). The clinical model was effective at separating the low- and high-risk patients in the training set ($P = 0.0032$). The median RFS for the training set was 17.2 months, while the 5-year % RFS was 83.4% and 28.6% for the low- and high-risk groups, respectively (Fig. 2A; Table 5). Nonetheless, application of a similar clinical model to the larger validation cohort was less successful ($P = 0.0518$; ref. 11). A genomic model developed from the training set was more effective than the clinical model at risk stratification of the training ($P < 0.0001$; Fig. 2A) and validation sets ($P < 0.0001$; Fig. 2B). Using the genomic model, the 5-year RFS for the low- and high-risk groups was 92.3% versus 15.4% and 67.5% versus 32.8% in the training and validation sets, respectively (Table 5). Using the clinicogenomic model, patients were effectively risk-stratified in the training ($P < 0.0001$) and validation sets ($P < 0.0001$; Fig. 2A and B). Using the clinicogenomic model, the 5-year RFS for the low- and high-risk groups was 92.3% versus 15.4% and 67.0% versus 33.3% for the training and validation sets, respectively (Table 5). In summary, the genomic and clinicogenomic models exhibit clinical utility because the difference in 5-year RFS is more than 2-fold indicating a substantial clinical effect.

Clinical, genomic, and clinicogenomic modeling of stage I and II patients in the validation set

Because the decision to offer chemotherapy or not is crucial for early stage patients, we reanalyzed the stage I to II patients in the validation set using the 4 genomic markers to develop genomic and clinicogenomic models for this risk group. The genomic model risk-stratified the stage I to II patients (P value < 0.0001 ; Fig. 2C), exhibiting 5-year RFS of 73.2% versus 33.8% for the low- and high-risk groups, respectively (Fig. 2C and Table 5). The clinicogenomic model also risk-stratified stage I to II patients (P value < 0.0001 ; Fig. 2C), exhibiting 5-year RFS of 69.6% versus 30.3% for the low- and high-risk groups, respectively (ref. Fig. 2C and Table 5). These results support the utility of the 4 genes for risk model development for stage I to II patients.

Genomic and clinicogenomic modeling of the validation set based on disease-specific OS

Risk stratification on the basis of disease-specific OS is another important test of the utility of the 4 genomic markers. Therefore, genomic and clinicogenomic models were developed. Both models were equally effective risk-stratifying the patients into low- and high-risk groups ($P < 0.0001$; ref. Fig. 3). Using the genomic and clinicogenomic models, the 5-year disease-specific survival for the low- and high-risk groups was 63.3% versus 37.0% and 67.3% versus 44.2%, respectively (Table 5). These differences in disease-specific OS were at least 1.5-fold, indicating clinical utility.

Table 4. qPCR analysis of *DBN1*, *CACNB3*, *FLAD1(PP591)*, and *CCND2*

Gene name	Relative % of expression			<i>P</i>
	Recurrent	Nonrecurrent	Fold change	
<i>DBN1</i>	50.7	24.2	2.094	0.012
<i>CACNB3</i>	82.1	28.1	2.921	0.033
<i>FLAD1(PP591)</i>	72	20.75	3.471	0.001
<i>CCND2</i>	189.9	405.79	0.468	0.058

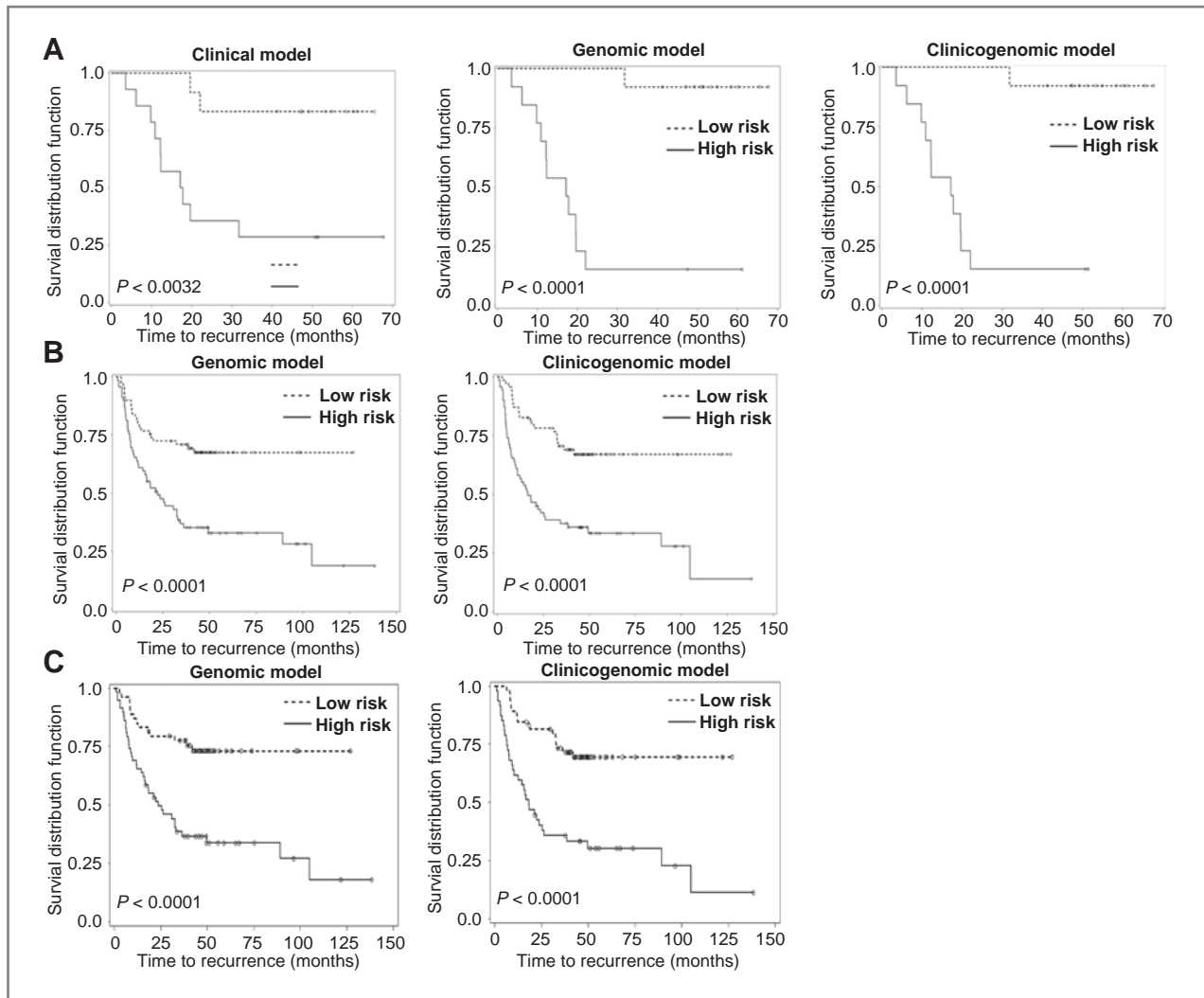


Figure 2. A, clinical, genomic, and clinicogenomic RFS models of training cohort (stage I–III patients). The clinical model is: Cox score = histology ($-16.12716 \times \text{squamous} - 1.03510 \times \text{other}$) + $0.95865 \times \text{pStage} + 0.22791 \times \text{gender} + \text{race} (-0.57444 \times \text{African American} - 0.95745 \times \text{undetermined})$; the genomic model is: Cox score = $-713.79613 \times \text{DBN1} - 1090 \times \text{CCND2} + 668.28496 \times \text{CACNB3} + 383.51066 \times \text{PP591}$; and the clinicogenomic model is: Cox score = $-1218 \times \text{DBN1} - 2072 \times \text{CCND2} + 1710 \times \text{CACNB3} + 507.39229 \times \text{PP591} + \text{histology} (-14.22074 \times \text{squamous} - 2.78616 \times \text{other}) + 0.60136 \times \text{pStage} + 1.40561 \times \text{gender} + \text{race} (-3.16002 \times \text{black} - 3.44106 \times \text{undetermined})$. The cutoffs (i.e., median Cox scores) for the clinical, genomic, and clinicogenomic models were 1.18655, -30.8891 , and -45.2830 , respectively. TTR is expressed in months; number of patients: 27. B, genomic and clinicogenomic RFS models of validation cohort (stage I–III patients). The genomic model is: Cox score = $0.38040 \times \text{DBN1} + 0.30160 \times \text{CACNB3} - 0.93964 \times \text{CCND2} + 0.28898 \times \text{FLAD1}$; the clinicogenomic model is: Cox score = $\text{pT stage} (0.58862 \times \text{T2} + 2.19489 \times \text{T3} + 0.31153 \times \text{T4}) + \text{pN stage} (0.75430 \times \text{N1} + 1.24674 \times \text{N2}) + 0.56392 \times \text{DBN1} + 0.43517 \times \text{CACNB3} - 0.61023 \times \text{CCND2} + 0.39543 \times \text{FLAD1}$. The median Cox scores for the genomic and clinicogenomic models were 3.66 and 7.43, respectively. TTR is expressed in months; number of patients: 138. The clinical model for this set of patients has been previously published (11). C, genomic and clinicogenomic RFS models of validation cohort (stage I–II patients). The genomic model is: Cox score = $0.37488 \times \text{DBN1} + 0.47831 \times \text{CACNB3} - 0.98259 \times \text{CCND2} + 0.33511 \times \text{FLAD1}$; the clinicogenomic model is: Cox score = $\text{pT stage} (0.82325 \times \text{T2} + 2.78736 \times \text{T3}) + 1.02786 \times \text{pN stage} + 0.54254 \times \text{DBN1} + 0.46196 \times \text{CACNB3} - 0.99139 \times \text{CCND2} + 0.36875 \times \text{FLAD1}$. TTR is expressed in months; number of patients: 112.

Analysis of multivariate marker *DBN1*

The genomic marker *DBN1* was identified as a significant in the genomic and clinicogenomic models of RFS stage I to III, RFS stages I to II, and disease-specific OS (stage I–III RFS genomic: HR = 1.463, CI = 1.088–1.967; stage I–III RFS clinicogenomic: HR = 1.758, CI = 1.248–2.476; stage I–II RFS genomic: HR = 1.455, CI = 1.038–2.04; stage I–II RFS clinicogenomic: HR = 1.72, CI = 1.165–2.541; OS geno-

mic: HR = 1.484, CI = 1.057–2.082; OS clinicogenomic: HR = 1.627, CI = 1.115–2.367; Supplementary Table S3). The addition of pT and pN stage information improved the significance of *DBN1* for all models (RFS stage I–III, $P = 0.0119$ – 0.0013 ; RFS stage I–II, $P = 0.0297$ – 0.0064 ; OS, $P = 0.0226$ – 0.0117). This finding indicates that *DBN1* serves as a component of the genomic model that can be improved by the addition of clinical stage.

Table 5. Cox modeling on the training and the validation set

	Clinical model		Genomic model		Clinicogenomic model	
	High risk	Low risk	High risk	Low risk	High risk	Low risk
Cox model training set (stage I-III)						
Median RFS time, months	17.167	∞	17.167	∞	17.167	∞
Survival percentage for 5 years, %	28.57	83.37	15.38	92.31	15.38	92.31
Cox model validation set (stage I-III)						
Median RFS time, months			21.40	∞	16.63	∞
Survival percentage for 5 years, %			32.80	67.46	33.32	66.95
Cox model validation set (Stage I-II)						
Median RFS time, months			23.77	∞	18.33	∞
Survival percentage for 5 years, %			33.84	73.19	30.33	69.56
Cox model validation set (OS; Stage I-III)						
Median disease-specific survival time (months)			22.40	∞	46.2	∞
Survival percentage for 5 years, %			36.91	63.31	44.23	67.35

NOTE: Clinical model of the validation set has been described in Lee and colleagues (11).

Discussion

We hypothesized that comparison of 2 geographically distant and demographically distinct patient cohorts, namely American and Korean, could facilitate the identification and validation of NSCLC genomic markers associated with RFS. Four genes were associated with recurrence in the American training set and validated in the larger Korean patient cohort. Genomic and clinicogenomic modeling for RFS risk-stratified both cohorts with high statistical significance, and genomic modeling alone was sufficient to risk-stratify the groups. Genomic and clinicogenomic models also risk-stratified stage I to II patients of the validation set. For stage I to II or I to III patients, the 5-year RFS of the low- and high-risk patients differed by 2-fold or more. The genomic and clinicogenomic models also predicted 5-year disease-specific OS, exhibiting a 1.5 to 1.7-fold difference between low- and high-risk groups.

The comparison of American and Korean cohorts resulted in discovery of *DBN1* as a multivariate biomarker, which by itself exhibits significant prognostic utility for RFS that is improved by the addition of the clinical markers of pT and pN stage. Because addition of clinical stage information increased the HR of the *DBN1* marker in all patient groups and for all outcomes, *DBN1* may be a platform on which to build future models consisting of other multivariate markers. Additional multivariate markers may be discovered by similar comparisons of demographically distinct NSCLC patient populations. For example, the validation set from this study could be used as the training set for an even larger demographically distinct patient cohort, such as a larger American patient group. This iterative process would confirm that some or all of the genomic markers derived here can

contribute to further model building, thus allowing model refinement.

It is notable that the genomic markers that correlate between the training and validation groups were not necessarily the ones exhibiting the lowest univariate *P* values for differential expression or the greatest fold-differences in expression. This indicates that if modeling were to be performed solely on the basis of *P* value or fold-differences, genes that could contribute to more robust modeling would be missed. Although clustering of gene expression patterns identified 4 clusters, only genes belonging to 3 of the clusters contributed to the model. Of note, one of these clusters contained 2 of the 4 genes, including *DBN1*, which is the only gene significant by multivariate analysis. The approach taken here suggests that successful genomic modeling can be performed even with a relatively small number of significant genomic markers identified by comparison of very different training and validation sets. Furthermore, the approach taken may be effective at identifying more reproducible and broadly applicable genomic markers, which are essential for efficient clinical trial development of a risk model. Thus, adopting this approach, a single, committed gene set can be derived that is statistically significant across a number of patient populations, independent of demographic factors, with informative Cox models as the product.

Of importance, the 4 genomic markers identified are all amenable to qPCR assay, which is an important factor in determining clinical development of the 4-gene set. The utilization of qPCR data for Cox model development confirms their robust amplification and indicates that the differences in their expression between recurrent and nonrecurrent patients is sufficient to overcome background noise (11). These findings also provide a robust assay to

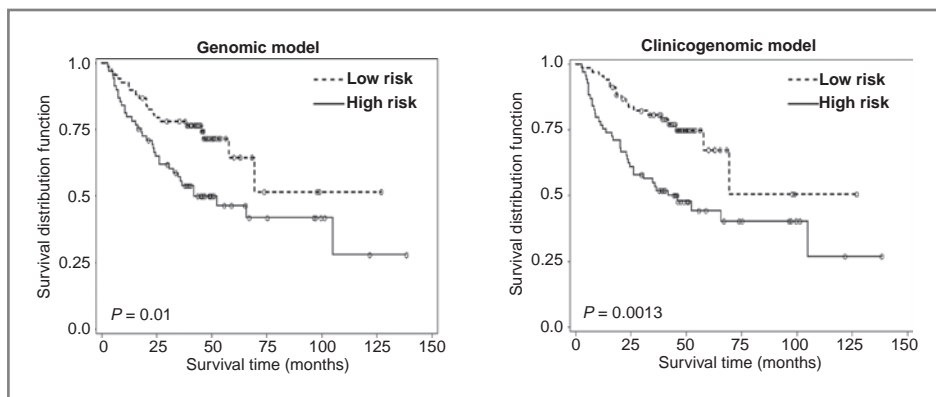


Figure 3. Genomic and clinicogenomic disease-specific OS models of validation cohort (stage I-III patients). The genomic model is: Cox score = $0.39443 \times \text{DBN1} + 0.13635 \times \text{CACNB3} - 0.77471 \times \text{CCND2} + 0.28103 \times \text{FLAD1}$; the clinicogenomic model is: Cox score = $\text{pT stage} (1.03717 \times \text{pT2} + 2.34391 \times \text{pT3} + 0.69257 \times \text{pT4}) + \text{pN stage} (0.54998 \times \text{pN1} + 1.22555 \times \text{pN2}) + 0.48697 \times \text{DBN1} + 0.25821 \times \text{CACNB3} - 0.69815 \times \text{CCND2} + 0.32732 \times \text{FLAD1}$. Overall survival is expressed in months; number of patients: 138.

allow rapid confirmation of the results in other NSCLC patient cohorts.

In summary, the genomic model developed in the present study identifies recurrence-associated genes that are internationally validated and are strong candidates for broader analysis in larger patient cohorts. The validated genomic model exhibits utility, because of the magnitude of the absolute differences between 5-year RFS and OS of the low- and high-risk patients. The utility of the 4-gene set is independent of stage, and is applicable to RFS of stage I to II, I to III patients as well as OS of stage I to III patients. Together these results support the further development of the 4-gene set or its multivariate *DBN1* component for future NSCLC risk model development. Of particular importance, risk-stratification has recently showed that low-risk NSCLC patients may exhibit decreased disease-specific survival when treated with adjuvant cisplatin/vinorelbine chemotherapy (1). With confirmation, our 4 genomic markers could be prospectively tested in a future clinical trial to determine the effectiveness of risk stratification of patients independent of stage and could also potentially be used to test the effectiveness of novel adjuvant chemotherapy regimens in low- and high-risk patients.

Disclosure of Potential Conflicts of Interest

No potential conflicts of interest were disclosed.

References

- Zhu CQ, Ding K, Strumpf D, Weir BA, Meyerson M, Pennell N, et al. Prognostic and predictive gene signature for adjuvant chemotherapy in resected non-small-cell lung cancer. *J Clin Oncol* 2010;28:4417-24.
- Beer DG, Kardia SL, Huang CC, Giordano TJ, Levin AM, Misek DE, et al. Gene-expression profiles predict survival of patients with lung adenocarcinoma. *Nat Med* 2002;8:816-24.
- Chen G, Gharib TG, Wang H, Huang CC, Kuick R, Thomas DG, et al. Protein profiles associated with survival in lung adenocarcinoma. *Proc Natl Acad Sci U S A* 2003;100:13537-42.
- Raponi M, Zhang Y, Yu J, Chen G, Lee G, Taylor JM, et al. Gene expression signatures for predicting prognosis of squamous cell and adenocarcinomas of the lung. *Cancer Res* 2006;66:7466-72.
- Yanagisawa K, Tomida S, Shimada Y, Yatabe Y, Mitsudomi T, Takahashi T. A 25-signal proteomic signature and outcome for patients with resected non-small-cell lung cancer. *J Natl Cancer Inst* 2007;99:858-67.
- Seike M, Yanaihara N, Bowman ED, Zanetti KA, Budhu A, Kumamoto K, et al. Use of a cytokine gene expression signature in lung

Acknowledgments

We thank Drs. Lawrence Einhorn, Nasser Hanna, David Flockhart, David Donner, Jorge Capdevila, Ming Sound Tsao, Ignacio Wistuba, David Beer, Mitch Raponi, Joan Schiller, Peter Ravdin, Faris Farassati, Janice Blum, Penni Black, Arkadiusz Dudek, and Miriam Garland for helpful discussions. We are grateful to Michael Franklin for outstanding editing help. This article is dedicated to the memory of Dr. Stephen Williams, past Director of the IU Simon Cancer Center whose vision led to the IU/Lilly Tumor Bank.

Grant Support

D.A. Potter acknowledges grants NIH P20GM066402, R01 CA113570, the Flight Attendant Medical Research Institute, Walther Cancer Research Prize, the Thoracic Oncology Program at Indiana University Simon Cancer Center, the Walther Oncology Center at Indiana University, the Cancer Experimental Therapeutics Initiative of the Masonic Cancer Center, and the Dr. Barbara Bowers Oncology Fund of the Fairview Foundation. The training set microarray experiments were carried out using the facilities of the Center for Medical Genomics at Indiana University School of Medicine, which is supported in part by a grant to H.J. Edenberg from the Indiana 21st Century Research and Technology Fund, and from the Indiana Genomics Initiative (INGEN). This work was supported in part by NIH P30CA077598 utilizing the support of the Biostatistics and Bioinformatics Core of the Masonic Cancer Center, University of Minnesota, shared resource. We acknowledge a grant from the Eli Lilly and Co. to support the tissue bank and Carol Boyd and Christina Beard for excellent technical help with tissue banking.

The costs of publication of this article were defrayed in part by the payment of page charges. This article must therefore be hereby marked *advertisement* in accordance with 18 U.S.C. Section 1734 solely to indicate this fact.

Received July 9, 2010; revised December 2, 2010; accepted January 3, 2011; published OnlineFirst January 17, 2011.

- adenocarcinoma and the surrounding tissue as a prognostic classifier. *J Natl Cancer Inst* 2007;99:1257–69.
7. Wright CD, Kesler KA. New trends in the surgical treatment of non-small cell lung cancer. *Indiana Med* 1990;83:192–4.
 8. Hanna N, Brooks JA, Fyffe J, Kesler K. A retrospective analysis comparing patients 70 years or older to patients younger than 70 years with non-small-cell lung cancer treated with surgery at Indiana university: 1989–1999. *Clin Lung Cancer* 2002;3:200–4.
 9. Ravdin PM, Davis G. Prognosis of patients with resected non-small cell lung cancer: impact of clinical and pathologic variables. *Lung Cancer* 2006;52:207–12.
 10. Mountain CF. Revisions in the international system for staging lung cancer. *Chest* 1997;111:1710–7.
 11. Lee ES, Son DS, Kim SH, Lee J, Jo J, Han J, et al. Prediction of recurrence-free survival in postoperative non-small cell lung cancer patients by using an integrated model of clinical information and gene expression. *Clin Cancer Res* 2008;14:7397–404.
 12. Potti A, Mukherjee S, Petersen R, Dressman HK, Bild A, Koontz J, et al. A genomic strategy to refine prognosis in early-stage non-small-cell lung cancer. *N Engl J Med* 2006;355:570–80.
 13. Kang CH, Ra YJ, Kim YT, Jheon SH, Sung SW, Kim JH. The impact of multiple metastatic nodal stations on survival in patients with resectable N1 and N2 nonsmall-cell lung cancer. *Ann Thorac Surg* 2008;86:1092–7.
 14. Kesler KA, Hammoud ZT, Rieger KM, Kruter LE, Yu M, Brown JW. Carinoplasty airway closure: a technique for right pneumonectomy. *Ann Thorac Surg* 2008;85:1178–85; discussion 85–6.
 15. Zhou FC, Duguid JR, Edenberg HJ, McClintick J, Young P, Nelson P. DNA microarray analysis of differential gene expression of 6-year-old rat neural striatal progenitor cells during early differentiation. *Restor Neurol Neurosci* 2001;18:95–104.
 16. McClintick JN, Jerome RE, Nicholson CR, Crabb DW, Edenberg HJ. Reproducibility of oligonucleotide arrays using small samples. *BMC Genomics* 2003;4:4.
 17. McClintick JN, Edenberg HJ. Effects of filtering by Present call on analysis of microarray experiments. *BMC Bioinformatics* 2006;7:49.
 18. Wu Z, Irizarry RA, Gentleman R, Martinez-Murillo F, Spencer F. A model-based background adjustment for oligonucleotide expression arrays. *J Am Stat Assoc* 2004;99:909–17.